Vol. 73: 167–186, 2017
https://doi.org/10.3354/cr01476

CLIMATE RESEARCH
Clim Res

Published online August 28

Spatially based reconstruction of daily precipitation instrumental data series

Roberto Serrano-Notivoli[1,2,3,*], Martín de Luis[1,3], Miguel Ángel Saz[1,3], Santiago Beguería[2]

[1]Department of Geography and Regional Planning, University of Zaragoza, Pedro Cerbuna 12, 50009 Zaragoza, Spain
[2]Estación Experimental de Aula Dei, Consejo Superior de Investigaciones Científicas (EEAD-CSIC), Avda. Montañana 1005, 50059 Zaragoza, Spain
[3]Environmental Sciences Institute (IUCA), University of Zaragoza, Pedro Cerbuna 12, 50009 Zaragoza, Spain

ABSTRACT: This work presents a method for the reconstruction of fragmentary daily precipitation datasets. The method aims to preserve the local and temporal variability characteristic of high-frequency precipitation data, and does not use the time-structure of the data. Based on the precipitation values recorded at closest neighbours during a target day, 2 reference values (RVs) are computed: a binomial prediction (BP) expressing the probability of occurrence of a wet day; and a magnitude prediction (MP), referring to the amount of precipitation. Generalised linear models (GLMs) are used to compute the RVs using the precipitation data (occurrence and magnitude) of the 10 nearest neighbours as the dependent variable, and the geographic information of each station (latitude, longitude, and altitude) as the independent variables. The RVs are then used to (1) apply quality control to the data, flagging suspect records according to 5 predefined criteria; (2) obtain serially complete time series by imputing RVs to missing observations in the original dataset; and (3) create new time series at locations where there were no observations or gridded datasets with even spatial coverage over the study area. The routines used were compiled into an R-package called 'reddPrec' (reconstruction of daily data – Precipitation) available to any user. We applied these methods to the complete daily precipitation dataset of the island of Majorca in Spain, spanning the period from 1971–2014.

KEY WORDS: Daily precipitation · Spatial analysis · Quality control · Missing values · Grid · ReddPrec

Resale or republication not permitted without written consent of the publisher

1. INTRODUCTION

Quality controlled and serially complete datasets are required in most climate studies in order to compute long-term climatologies, to assess the existence of trends, for statistical downscaling of global and regional climate model data, or to analyse the frequency and magnitude of extreme events, to name a few topics. Great effort has been expended to create datasets of climatic variables at different temporal resolutions, with spatial coverage ranging from the global scale (New et al. 1999, 2000 , 2002, Hijmans et al. 2005, Mitchell & Jones 2005, Lawrimore et al. 2011, Becker et al. 2013) to the regional or local scale (Klein-Tank et al. 2002, Perry & Hollis, 2005, Ninyerola et al. 2007, Li et al. 2009, Vicente-Serrano et al. 2010, González-Hidalgo et al. 2011, Herrera et al. 2012, Chaney et al. 2014). These datasets address a growing demand for climate data, in order to understand the climate behaviour of the past and to serve as a basis for making reliable estimations of its future evolution (Trenberth 2011, Zhang et al. 2011, Zwiers et al. 2013, Trenberth et al. 2014).

Among all the variables for which datasets have been created, precipitation is one of the most elusive, because of its considerable temporal and spatial vari-

*Corresponding author: rs@unizar.es

© Inter-Research 2017 · www.int-res.com

ability. Most studies focusing on creating climatologies or determining trends in precipitation use datasets at a monthly time resolution (New et al. 1999, 2000, 2002, Mitchell & Jones 2005, Perry & Hollis 2005, Norrant & Douguédroit 2006, Caramelo & Manso 2007, Ninyerola et al. 2007, González-Hidalgo et al. 2011, Río et al. 2011). While a monthly scale may be acceptable for climatological studies focused on precipitation totals, it is not sufficient for other crucial issues such as extreme event analyses (which usually involve heavy impacts), for which daily or even higher time resolutions are necessary (Zhang et al. 2011). However, the development of high-frequency precipitation datasets poses a number of difficulties that limit their more widespread use. The increase in the amount of data compared to the monthly scale, the comprehensive quality control needed, and the high variability of the spatial fields requires considerable effort in terms of process automation and computing time. Quality-control and reconstruction methods developed for monthly data perform well for computing long-term averages or assessing trends in precipitation totals, and take advantage of the higher spatial correlation of the data at low time-resolutions. However, such procedures cannot be applied to daily-scale precipitation data due to the much higher spatial variability and the interaction of local issues such as orography, which, in combination with specific atmospheric conditions, can lead to variability in spatial distribution patterns from one day to the next. These issues have caused daily precipitation to be one of the least studied variables in climate reconstruction studies, despite its great importance in extreme event analysis (Easterling et al. 2000, Griffiths et al. 2003, Alexander et al. 2006, López-Moreno et al. 2010, Min et al. 2011, Beguería et al. 2011, Orlowsky & Seneviratne 2012).

Several studies have described daily precipitation reconstructions as a means to reach other objectives. Some of them created climatologies by direct estimation of precipitation in grid points from raw data (Frei & Schär 1998) or by avoiding quality control and considering only elevation parameters (Daly et al. 2002). Other works were based on interpolation of the anomalies from the climatological normal (Schneider et al. 2014), or improving downscaling methods (Wong et al. 2014). Different climatological studies based their analyses on daily precipitation values, but few of them (Feng et al. 2004, Vicente-Serrano et al. 2010, Castro et al. 2014) included complete quality control of the information used. In addition, most of the methods are based on the selection of a reduced number of stations (those whose datasets are longer and expected to be of higher quality), rejecting data of potential value.

Similar limitations can be found in different approaches used to create global or regional daily precipitation datasets. For instance, Eischeid et al. (2000) used only series with a minimum length and selected neighbouring stations by correlation, smoothing the local variability of precipitation. In a first version of the European Climate Assessment Dataset, Klein-Tank et al. (2002) applied quality control by considering only the temporal structure of the series. Later, Klok & Klein-Tank (2009) updated this dataset by adding stations, but they did not apply spatial quality control and did not do any kind of reconstruction, similar to the work of Menne et al. (2012) for a global dataset.

Substantial effort has been invested in the creation of daily gridded datasets. However, most of the previous works addressed (1) problems of loss of spatial resolution due to the use of monthly totals in the estimation of daily precipitation (Haylock et al. 2008, Yatagai et al. 2012); (2) the selection of series with a minimum length combined with global models in interpolation schemes (Herrera et al. 2012) that produced smoothed estimations with a low number of zeros and underestimated maximum events; or (3) the application of homogenisation procedures to reanalyse products (Chaney et al. 2014).

Other works tested methods to estimate daily precipitation for use in climatology (Neykov et al. 2014) and hydrology (Hwang et al. 2012), addressing similar problems of sub-optimal use of available data due to the need for the correlation of series (Verdin et al. 2015, Kleiber et al. 2012), and the incorporation of the error term in final estimations by using monthly empirical cumulative distribution functions (Clark & Slater 2006). All of these approaches restrict the resolution and local results of daily precipitation datasets.

Only a few studies have focused specifically on quality control and reconstruction of daily precipitation (Feng et al. 2004, Simolo et al. 2010, Vicente-Serrano et al. 2010, Castro et al. 2014). The creation of these datasets typically involves a process including quality-control tests for detecting and eliminating suspect data, correcting inhomogeneities within the data, and reconstructing fragmentary series. Reference series (RS) are commonly used in all these stages. A common characteristic of RS calculation is the use of data from neighbouring stations. However, the construction of RS requires that both candidate and neighbour series are long enough and overlap over a significant period. This is problematic, as short

or non-overlapping data series must be rejected from the final dataset, making sub-optimal use of the available information. Besides, 2 important assumptions are necessary for the construction of RS: (1) that the relationship among neighbour series does not vary over the reference period and/or during the overlap period of the 2 series; and (2) that the series have a similar temporal structure throughout the period. These are problematic assumptions, especially with daily data, since the behaviour of neighbouring stations may be very different on daily scales, and because the evolution of precipitation can differ between nearby locations.

The purpose of this paper is to present a spatially-based method for daily precipitation reconstruction that preserves both spatial and temporal variability. This approach is made without any preconceived assumptions about the structure of the series or their relationship with nearby series, and by maximising the use of available information. This method can be used to (1) apply quality control to daily precipitation datasets; (2) reconstruct missing values; and (3) estimate precipitation values at specific locations of interest, even if no direct observations exist. All calculations were made in the R language (R Core Team 2016), using a new package called 'reddPrec' (reconstruction of daily data – Precipitation) that was compiled with all the required functions, and made available to any interested user (Serrano-Notivoli et al. 2017).

The approach was tested and validated using daily precipitation data series from the island of Majorca in Spain. Located in the western Mediterranean, its orographic diversity (altitudes ranging between 0 and 1445 m a.s.l.) produces a varied climate subject to many influences. The island has an irregular and torrential precipitation regime, including long periods of consecutive dry days and frequent extreme precipitation events. In addition, the rain gauge network is relatively dense in space but strongly variable in the duration and expected quality of the series, representing a perfect framework to validate a daily precipitation reconstruction method.

2. DESCRIPTION OF THE METHOD AND CASE STUDY

2.1. Reference values as a general tool for quality control and reconstruction

The key difference between the method proposed here and others traditionally used is the use of individual reference values (RVs), instead of RS, to complete the quality control during the reconstruction process.

RVs are calculated independently for each day and location according to the available data for that day from close neighbouring stations. The geographic data of each station (latitude, longitude, and altitude) are used as the independent variables for modelling. Since data availability varies from day to day, selected neighbour stations can also vary accordingly. Also, since independent models are constructed for each location and day, the estimated parameters of the models (reflecting the influence of the altitude, latitude, and longitude on the probability of occurrence and the magnitude of precipitation) may also vary in their sign and magnitude from neighbouring stations, or over different days for the same location. Such an approach, including 3 regressors, allows the creation of highly flexible models able to reflect local precipitation conditions. In addition, since neighbour selection is local and independently determined each day, no restriction on data selection according to dataset length or structural characteristics exists, allowing use of all available information.

Generalised linear models (GLMs) are used to compute the RVs using the precipitation data (occurrence and magnitude) of the 10 nearest neighbours as the dependent variable, and the geographic information of each station (latitude, longitude, and altitude) as the independent variables.

Computation of each individual RV is based on 2 predicted values: (1) a binomial prediction (BP) of the probability of occurrence of a wet day; and (2) the magnitude prediction of precipitation (MP). Both are calculated with a multivariate logistic regression that uses topographic and geographic characteristics of the stations as independent variables:

$$P_{i,l} = \beta_{0_{i,l}} + \beta_{1_{i,l}} alt_l + \beta_{2_{i,l}} lat_l + \beta_{3_{i,l}} lon_l + \varepsilon_{i,l} \quad (1)$$

where $P_{i,l}$ is the BP or the MP on day i and at location l; $\beta_{n_{i,l}}$ are the regression coefficients; *alt*, *lat*, and *lon* are the altitude, latitude, and longitude, respectively, of the 10 nearest neighbour stations (NNS) with observations on that day; and $\varepsilon_{i,l}$ is the error term. The equation is least-squares fitted, based on the data. R-language nomenclature is used to describe the RV computation (R Core Team 2016). The function 'glm' from R-package 'stats' is used to calculate both BP and MP (Serrano-Notivoli et al. 2017).

The probability of occurrence of precipitation on day i at location l ($BP_{i,l}$) is computed by using the binomial family (Eqs. 2, 3, & 4) to describe the error distribution (equivalent to a logistic regression):

$$\text{modelBP}_{i,l} = glm(\text{PCPb} \sim \text{ALT} + \text{LAT} + \text{LON}, \text{data} = \text{NEI}, \text{family} = \text{binomial}) \quad (2)$$

$$\text{BP}_{i,l} = \text{predict}(\text{modelBP}_{i,l}, \text{newdata} = \text{CAN}, \text{type} = \text{"response"}) \quad (3)$$

$$err_{i,l} = \frac{\sqrt{\text{sum}\left(\text{PCPb} - \text{BP}_{i,l}\right)^2}}{\text{length}(\text{PCPb}) - 3} \quad (4)$$

where PCPb contains information on whether the day was dry or wet (codified as 0 or 1, respectively) in the 10 NNS that collected precipitation during day i ($\text{NNS}_{i,l10}$); and ALT, LAT, and LON are the vectors containing the geographic locations of these neighbouring stations. The $modelBP_{i,l}$ is then applied to the ALT, LAT, and LON of the candidate station l to calculate the probability of occurrence of precipitation on day i ($\text{BP}_{i,l}$). The uncertainty of $\text{BP}_{i,l}$ is also computed at each step as described in Eq. (3). PCPb and the ALT, LAT, and LON of the neighbouring stations are stored in the dataframe NEI while the geographic information of candidate station l is stored in dataframe CAN.

Similarly, the MP of precipitation on day i and location l ($\text{BP}_{i,l}$) is also computed using the *glm* function, but now using the quasi-binomial family to describe the error distribution (Eqs. 5, 6, & 7):

$$\text{modelMP}_{i,l} = glm(\text{PCPq} \sim \text{ALT} + \text{LAT} + \text{LON}, \text{data} = \text{NEI}, \text{family} = \text{quasibinomial}) \quad (5)$$

$$\text{MP}q_{i,l} = \text{predict}(\text{modelMP}_{i,l}, \text{newdata} = \text{CAN}, \text{type} = \text{"response"}) \quad (6)$$

$$err_{i,l} = \frac{\sqrt{\text{sum}\left(\text{PCPq} - \text{MP}_{i,l}\right)^2}}{\text{length}(\text{PCPq}) - 3} \quad (7)$$

where PCPq includes the precipitation magnitudes observed for day i at the 10 nearest stations (Obs) rescaled between 0 and 1, with 0 being half of the minimum precipitation observed (Obsmin), and 1 being the maximum value (Obsmax) plus the difference between the maximum and minimum, minus half of the minimum (Eq. 8). This rescaling of the data in a quasi-binomial model context allows the fixing of asymptotic limits to the predicted values according to the range of the local variation of observations. This transformation is especially useful in situations where the geographic conditions of the candidate stations are out of the range of altitudes, latitudes, or longitudes of its NNS. Finally, the predicted value $\text{MP}q_{i,l}$ is rescaled inversely (Eq. 9) to obtain the final precipitation magnitude prediction ($\text{MP}_{i,l}$):

$$\text{PCPq} = \frac{(\text{Obs} - 0.5 \times \text{Obsmin})}{(2 \times \text{Obsmax} - \text{Obsmin}) - 0.5 \times \text{Obsmin}} \quad (8)$$

$$\text{MP}_{i,l} = \text{MP}q_{i,l} \times [(2 \times \text{Obsmax} - \text{Obsmin}) - 0.5 \times \text{Obsmin}] + (0.5 \times \text{Obsmin}) \quad (9)$$

$$\text{PCPq}_{i,l} = \text{Obs}_i - 0.5 \times \text{Obsmin} \quad (10)$$

The final RV is determined by combining MP and BP (See Table S1 in the Supplement at www.int-res.com/articles/suppl/c073p167_supp.pdf), using a threshold value of $\text{BP}_{i,l} \geq 0.5$ to determine a wet day:

$$\text{RV} = \begin{cases} \text{MP} & \forall\ \text{BP} \geq 0.5 \\ 0 & \forall\ \text{BP} < 0.5 \end{cases} \quad (11)$$

The threshold of 0.5 allows the sum of the probabilities of occurrence of the predicted wet days in that area to be equal to the observed occurrence of that situation. For instance, given an area defined by 10 stations where precipitation occurred at 7 of them (70% wet stations), the model assigns 70% of the area associated with these stations with probabilities of >0.5, and 30% of the area with probabilities <0.5.

2.1.1. Potential for quality control

The RV can be used to develop a quality control (QC) test to detect anomalous data. There are numerous different reasons to expect that anomalous or erroneous data are present in original climate datasets, including codification errors, incorrect transcriptions from manual to digital data, reading errors from analogue devices, problems in software or hardware at automatic stations, and many more (Reek et al. 1992, Feng et al. 2004, Su-Ping et al. 2012). For this reason, a comprehensive analysis of the data from each station on each day is necessary to be certain that the final dataset will be consistent and reliable. RVs, calculated as described in the previous section, were used to perform a QC of the original values. To do this, RVs were calculated for each individual observed precipitation value and 5 criteria were defined to identify suspect values: (QC.1) isolated wet conditions: observed value is over zero and the precipitation at the 10 nearest neighbouring stations that measured precipitation during the same day ($\text{NNS}_{i,l10}$) is zero. (QC.2) Isolated dry conditions: observed value is zero and all 10 $\text{NNS}_{i,l10}$ are over zero. (QC.3) Suspect outlier: the magnitude of the observed value is 10 times higher or lower than that predicted by its 10 $\text{NNS}_{i,l10}$. A value of 1 mm was added to each element to avoid conflicting situations

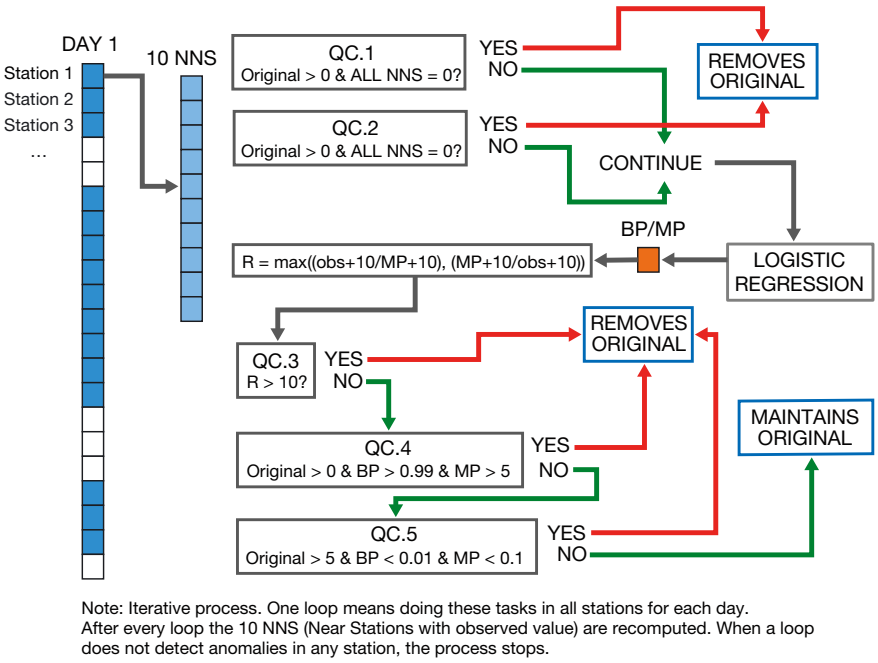

Fig. 1. Workflow of quality control process. BP: Binominal Prediction; MP: Magnitude Prediction

when computing with zero values. (QC.4) Suspect dry: observed value is zero, wet probability is over 99%, and predicted magnitude is over 5 mm. (QC.5) Suspect wet: observed value is over 5 mm, dry probability is over 99%, and predicted magnitude is under 0.1 mm.

The 5 QC criteria were applied to all observed data and the suspect observations were removed. This process was repeated using the cleaned database from the previous step until no more observations were flagged (Fig. 1).

2.1.2. Potential for gap filling

The RVs can also be used for gap filling in order to obtain serially complete data series. In this case, the RVs can be directly used to fill in the missing values. To preserve the peculiarities of the original series and to avoid including inhomogeneity in the time dimension, a correction is required consisting of multiplying the RV by a correction coefficient computed as the ratio between the monthly means of daily precipitation of all observed values, and the same calculation of predicted data. This allows RV series to have the same mean as that of the observed data in the candidate series. Correction coefficients are computed for each monthly value independently to avoid biases due to seasonal variation:

$$\mathrm{RV}c_{i,m} = \mathrm{RV}_{i,m} \times \left(\overline{\mathrm{Obs}_m} / \overline{\mathrm{RV}_m}\right) \quad (12)$$

To compute the corrected value for day i of a specific year, the RV of the same day, $\mathrm{RV}_{i,m}$, is multiplied by the ratio between the average of the observations in that month for all lengths of the series, Obs_m, and the average of the estimations of that month in the same period, RV_m.

2.1.3. Potential for inference

The computation of the RV can also be used for estimating precipitation values at locations where no direct observations exist. Using the coordinates and altitude of the location of interest, and based on the observations at the 10 NNS, complete daily precipitation series can be computed. This is useful for creating new data series at single, ungauged locations, and it can also be used for computing gridded datasets by applying the same approach to a set of regularly distributed pairs of coordinates.

The process of inferring a new series is the same as that used to fill missing values in the original series. In the first stage, all the data series with observations are filled. As the new estimations cannot be corrected by the original values (because there are no observations at the candidate location), they need to use the same 10 NNS each day to avoid including inhomogeneity. In a second stage, the new RVs are computed for each day using the filled original stations. These RVs are the final estimations.

2.2. Software implementation

An R package called 'reddPrec' (reconstruction of daily data – Precipitation) was developed containing the previously described procedures. This package contains 2 main functions: 'qcPrec' flags suspect data, as explained in Section 2.1.1., resulting in a cleaned dataset; and 'gapFilling' computes the RV to fill missing data (Section 2.1.2.) and/or create new series (Section 2.1.3.), depending on the set of locations included as input. The package is freely available from the official R repository (http://cran.r-project.org/web/packages/reddPrec/index.html); its operation is explained in Serrano-Notivoli et al. (2017).

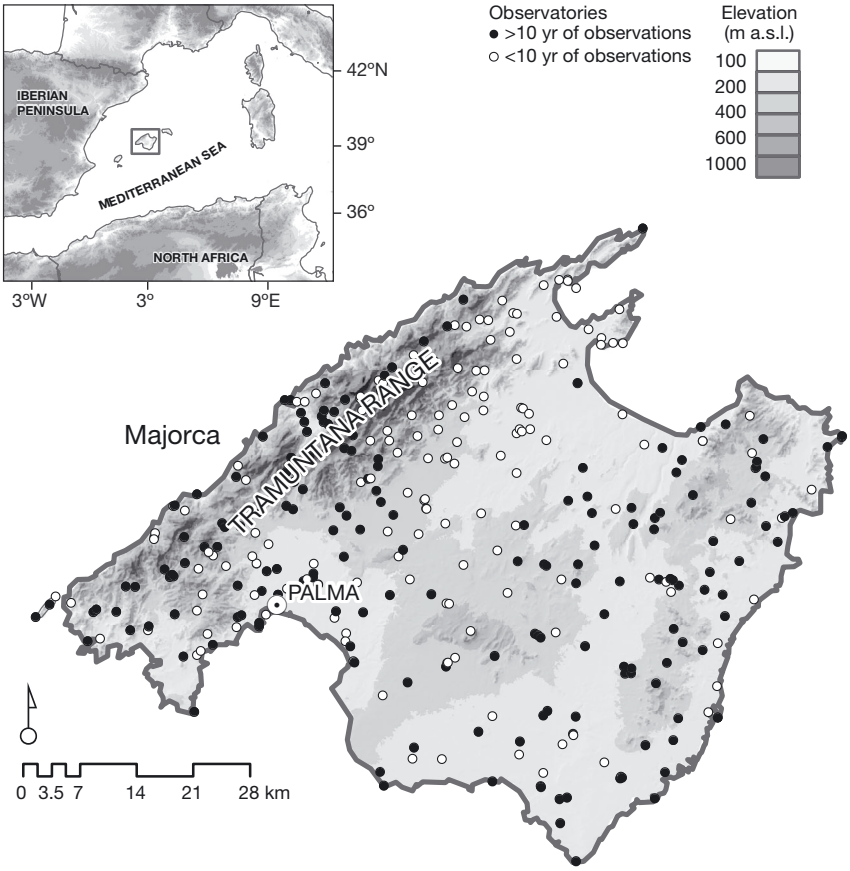

Fig. 2. Spatial structure of the daily precipitation dataset: location of the stations (dots) used in this study

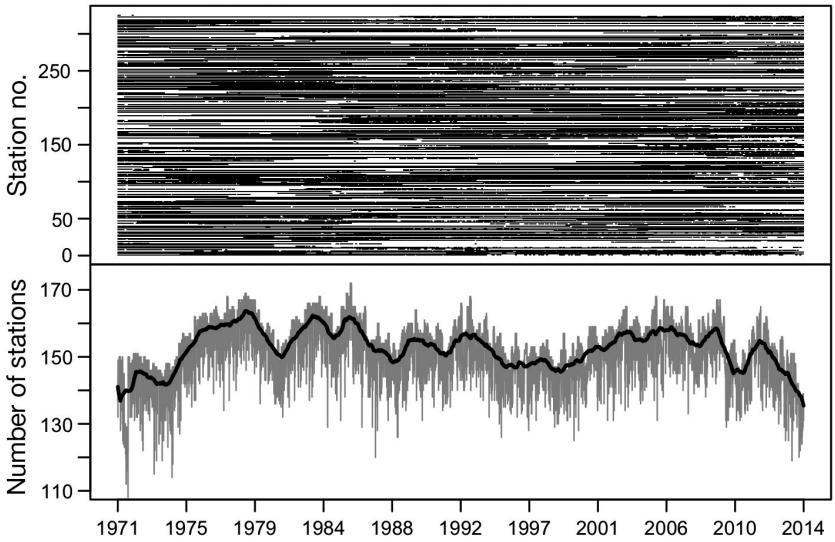

Fig. 3. Temporal structure and evolution of the daily precipitation dataset. Upper panel: black lines indicate the days with observed data in each station. In an ideal situation with no gaps in observations, a black surface will be shown. Lower panel: number of daily available data (grey lines) and 365 d moving average (black line)

2.3. Case study: evaluating the accuracy of the reconstruction process

The method was evaluated using all available precipitation data covering the island of Majorca for the period between 1971 and 2014 (Fig. 2). The purpose of the validation was to evaluate the agreement between the observations registered in these stations and their corresponding predictions, computed for each location and time of observed values.

In Majorca, most rainfall occurs during the autumn, and from November to April it is generally associated with the Atlantic Westerlies and other cyclogenetic processes within the western Mediterranean Basin (Sumner et al. 1995a). Convective storms are more frequent in the warmer season. Intense precipitation events mostly occur from September to November (Sumner et al. 1995a). Annual precipitation is >1000 mm in the highest zones of the Tramuntana Range and falls gradually with altitude to amounts <400 mm in the south-east coastal fringe (Sumner et al. 1995b).

During the period 1971–2014, a total of 325 precipitation stations existed in Majorca. Of these, only 2.8% registered >99% of the daily observations during the whole period, and a total of 216 stations included data from >10 yr. The average length of time series is 21 yr, and the number of stations available on any day ranges from 110–170 (Fig. 3, lower panel). Globally, data gaps accounted for 53.05% of the original dataset, and they were regularly distributed over time, not focused in a specific season or group of years (Fig. 3, upper panel).

The data from the 325 stations were subjected to QC and all the suspect data were flagged and discarded before further analysis. Gap filling was performed by imputing the RVs for any missing data. Finally, the set

of 216 stations with >10 yr of original data were reconstructed and used to build a 1 × 1 km grid across the island.

The accuracy of the reconstruction method was evaluated based on 3 different statistical analyses: (1) a contingency table analysis was used to assess the accuracy of the binomial (wet/dry) prediction. Accuracy was computed for global observation–estimation comparison, and separated by month. (2) A correlation analysis between observed and predicted data allowed comparison of the RVs and observations in 2 ways: (i) using daily results, the correlation between observations and predictions of daily precipitation means (considering all days) was calculated for each day, medians of the wet days, and the 95th percentile of the wet days; and (ii) using the same methods but applied to each station. (3) Goodness-of-fit (GOF) was assessed through 4 different statistics: the mean absolute error (MAE), mean error (ME), ratio of means (RM), and ratio of standard deviations (RSD). The MAE is calculated as the mean of the absolute differences between predicted and observed values, and provides information about the magnitude of the errors irrespective of their sign:

$$\mathrm{MAE} = \frac{1}{n}\sum_{i=1}^{n}\left|p_i - o_i\right| \tag{13}$$

where p is the predicted value; o is the observed value, and n is the number of cases. The ME is the mean of the differences between predicted and observed values, and gives the bias (the tendency towards under- or over-predicting):

$$\mathrm{ME} = \frac{1}{n}\sum_{i=1}^{n}\left(p_i - o_i\right) \tag{14}$$

These statistics were applied to daily values by splitting the whole dataset (only observations over zero) into deciles according to the distribution of observed values, as well as to monthly aggregated values (only considering predicted values for available observations) in order to check the performance of the method for aggregated precipitation.

Finally, the RM and the RSD were performed. These techniques give the bias on the estimation of the mean and the variance of the data, with a value of 1 indicating a non-biased estimate:

$$\mathrm{RM} = \frac{\bar{p}}{\bar{o}} \quad \mathrm{RSD} = \frac{\sigma_p}{\sigma_o} \tag{15}$$

where $\bar{p}$ is the mean of estimates, $\bar{o}$ is the mean of the observations, σ_p is the standard deviation of the predictions, and σ_o is the standard deviation of the observations. These 2 statistics were applied only to monthly and annual totals, since the distribution of the daily precipitation data is highly non-normal, so these techniques would be misleading in that case.

Daily precipitation climatologies were developed by computing several indices at the annual scale to assess the accuracy of the spatial distribution of climatic variables. They were analysed through the annual total precipitation, daily precipitation intensity (PMED), maximum precipitation in 1 d (RX1), number of days with precipitation >20 mm (R20mm), maximum consecutive dry days (CDD), and maximum consecutive wet days (CWD). These variables were mapped using the grid computed at a 1 × 1 km spatial distribution based on the reconstructed stations.

3. RESULTS

3.1. Quality control

From the 2 412 810 original daily precipitation observations, 1.59% were flagged (and removed) according to the rules outlined in Section 2.1.1. The rate of flagged data was higher during the first 20 yr when data availability was lowest (Fig. 4a). QC.2 (isolated dry conditions) was the most frequent criterion (34.8% of total), especially in the first 15 yr and during the months with a larger number of wet days (in winter and spring; Fig. 4b). These high values are probably due to days when the accumulated precipitation does not reach the minimum to be noted (if the observation is taken manually) or detected (if at an automatic station). QC.1 (isolated wet conditions) was more evenly distributed over the period and was also a large source of flagged data (23.2%). This precipitation probably occurred, but the climatic context suggests that it is far from representative of the local climatic situation, and most of the removed data were low values (Fig. 4c). The frequency of flagged data due to QC.4 (suspect dry) (20.5%) and QC.5 (suspect wet) (12.5%) decreased from the start to the end of the time series. They represent similar situations to QC.2 and QC.1, respectively, by removing mainly zero or low precipitation values when predicted values were very low in the case of QC.4 (Fig. 4e) and removing values under 20 mm in almost all cases with QC.5 (Fig. 4f). QC.3 (suspect outlier) (9%) represented the detection of outliers. These outliers were observations that differed from predictions by an order of magnitude, and were probably due to codification problems and confusion with decimal places, which produces the removal of a great num-

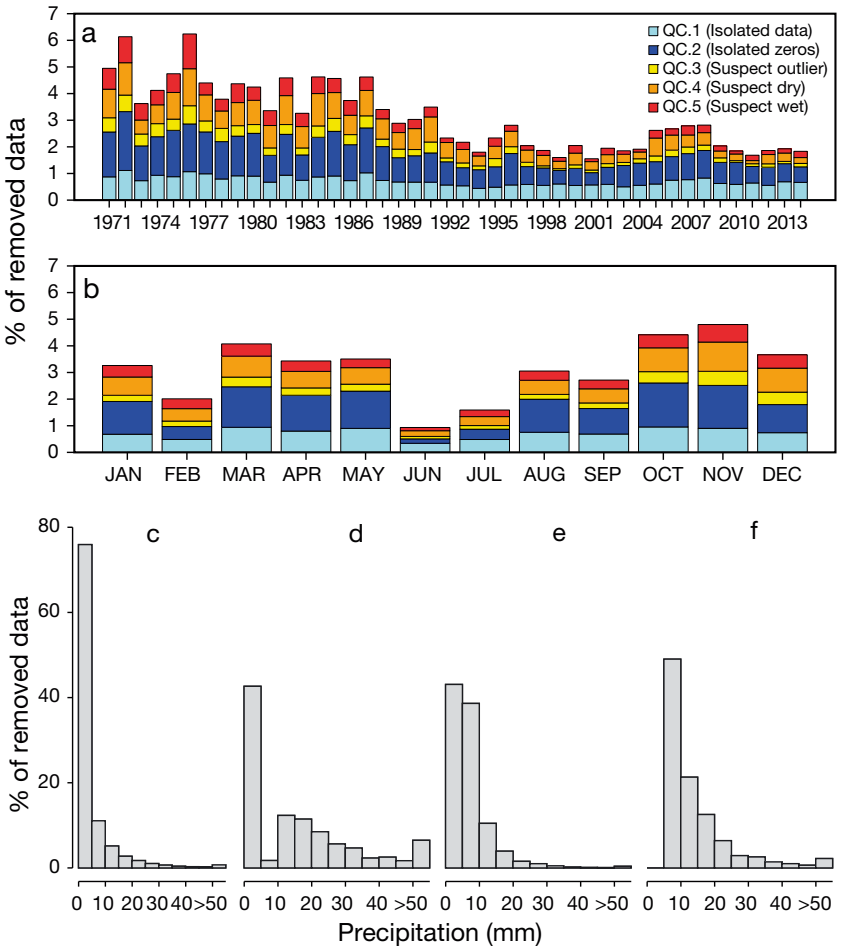

Fig. 4. Quality control (QC) results. (a) Annual and (b) monthly percentage of removed data using the 5 QC criteria (stacked bars). Frequency distribution of observations removed by (c) QC.1 (isolated wet conditions), (d) QC.3 (suspect outliers), and (f) QC.5 (suspect wet). (e) Frequency distribution of estimations used to remove observations by QC.4 (suspect dry)

ber of low values (Fig. 4d). However, a wide range of daily precipitation values were flagged as suspect. For instance, high extremes (>50 mm) represented 6.5% of removed data in this category, and their inclusion in this category represented situations where the observed value was very different from that predicted by its nearest neighbours. QC.3 was more frequent in months with intense precipitation (October to December), but it was lower in the warmer season, when it is expected that more convective storms will occur (Fig. 4b). This means that the quality control process is more sensitive to extreme precipitation than to regular convective situations.

3.2. Agreement between observed and predicted precipitation values

3.2.1. Wet/dry prediction

The percentage of true and false positives and negatives of predictions gives information about the accuracy of the wet and dry day prediction (Fig. 5a, Table 1). A rate of 82.84% of true positives, representing the correctly predicted wet days, was obtained. The false positives corresponded in most cases with low values (median: 1.2 mm; mean: 2.2 mm), with the BP in most of these cases near 0 but also >0.5 (Fig. 5a,c). The rate of true negatives, representing well-predicted dry days, was very high (96.36%).

False negatives (wet predictions on dry days) were identified in 3.58% of observed dry days (median: 0.99; mean: 1.7 mm) but only in 0.22% of cases did MPs exceed 5 mm, BP values being higher than 0.5 in a few cases (Fig. 5b,d). The accuracy of the wet/dry prediction by month (Table 1) showed that overall, the percentage of well-predicted dry days was

Table 1. Contingency table with the percentage of true and false zero and positive. True zero: predicted and observed precipitation values are zero. False zero: observed value is zero but predicted value is positive. True positive: predicted and observed precipitation values are positive. False positive: observed value is positive but predicted value is zero

	True zero (%)	False zero (%)	True positive (%)	False positive (%)
All	96.36	3.58	82.84	17.16
Jan	95.37	4.63	84.45	15.55
Feb	94.96	5.04	83.47	16.53
Mar	95.88	4.12	82.70	17.30
Apr	95.37	4.63	82.00	18.00
May	96.94	3.06	82.00	18.00
Jun	98.25	1.75	77.70	22.30
Jul	99.06	0.94	70.78	29.22
Aug	98.41	1.59	78.15	21.85
Sep	96.77	3.23	84.06	15.94
Oct	95.33	4.67	84.42	15.58
Nov	94.62	5.38	84.86	15.14
Dec	94.13	5.87	82.54	17.46

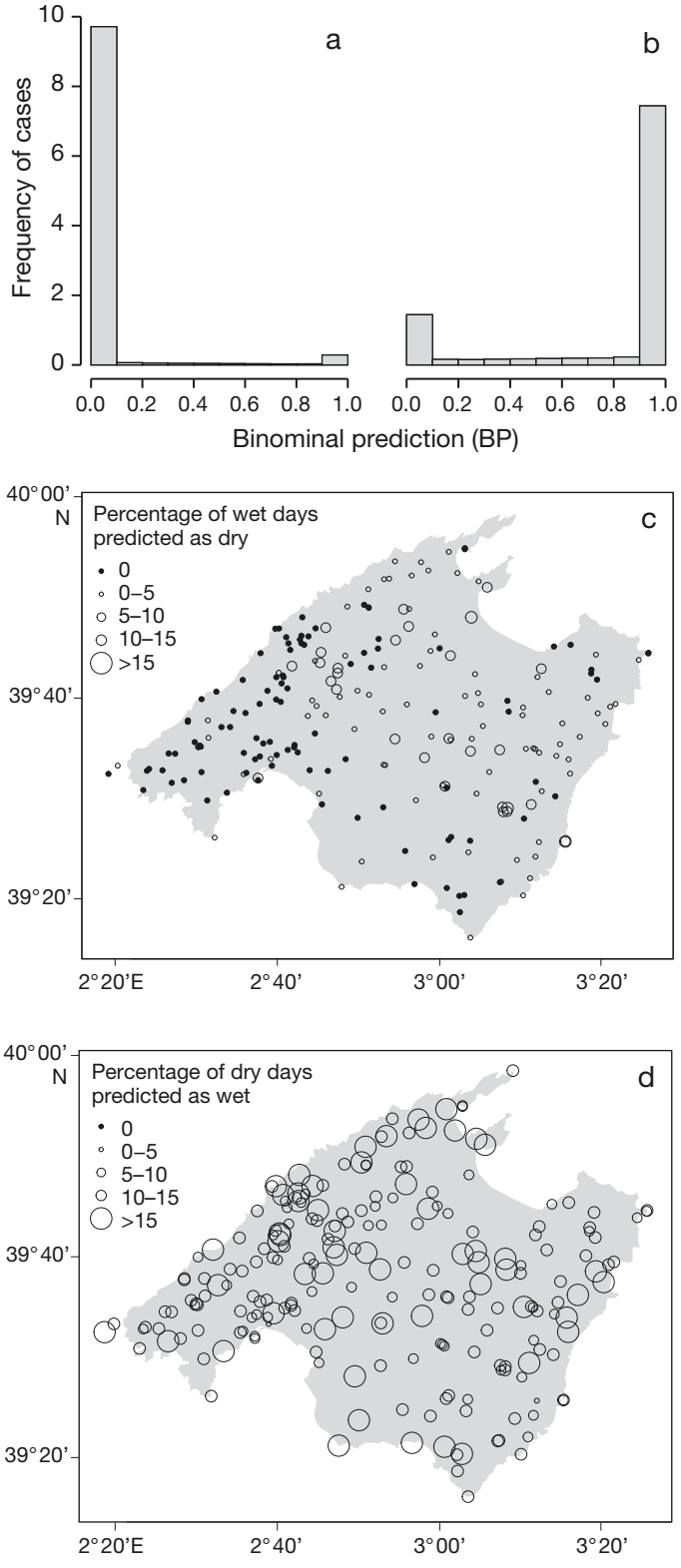

Fig. 5. Frequency distribution of binomial predictions of occurrence of precipitation (BP) on (a) dry and (b) wet days and spatial distribution of percentage of (c) wet days estimated as dry and (d) dry days estimated as wet

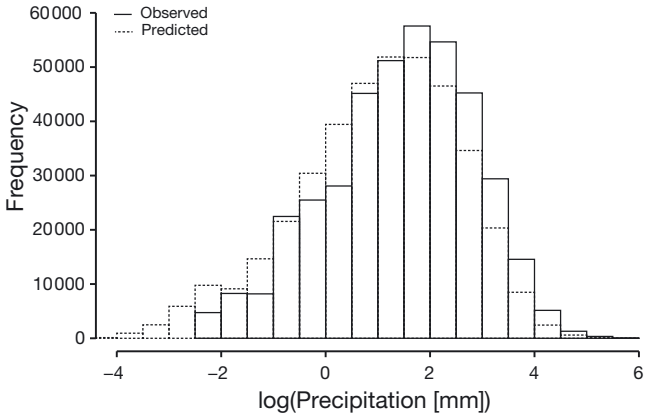

Fig. 6. Frequency distribution of observations and estimations (days with zero in observations and estimations are not shown). Precipitation classes are created in logarithmic scale

higher than the well-predicted wet days that obtained values under 80% in summer months (Jun, Jul, and Aug).

3.2.2. Magnitude prediction

Overall, the distribution of observations and predictions was very similar, with a slight overestimation of the lowest values and underestimation of the highest (Fig. 6). However, predictions of lower values were more frequent, showing a global displacement that is not reflected in correlations when aggregating by daily means (Pearson's r = 0.999; Fig. 7a). This strong correlation is influenced by the prevalence of days with no precipitation in the dataset. However, even considering only the wet days, the agreement between RVs and observations was also high (r = 0.992). Similar results were obtained when days with precipitation exceeding the 95th percentile were considered (r = 0.991). The density curves constructed for observed and predicted values also show a highly significant agreement (Fig. 7d–f). Overall, there were discrepancies in the low values, showing a slight overestimation in estimated values. This is mainly due to the higher number of observations with low values.

By analysing the same statistics when averaging precipitation by stations instead of days, quite high correlations were also obtained (r > 0.96 in all cases; Fig. 8), and the density curves of predicted values matched those of the observed values quite well.

The comparison between observed (%OBS) and predicted (%PRED) data by deciles showed small differences (Table 2). These values are related to the

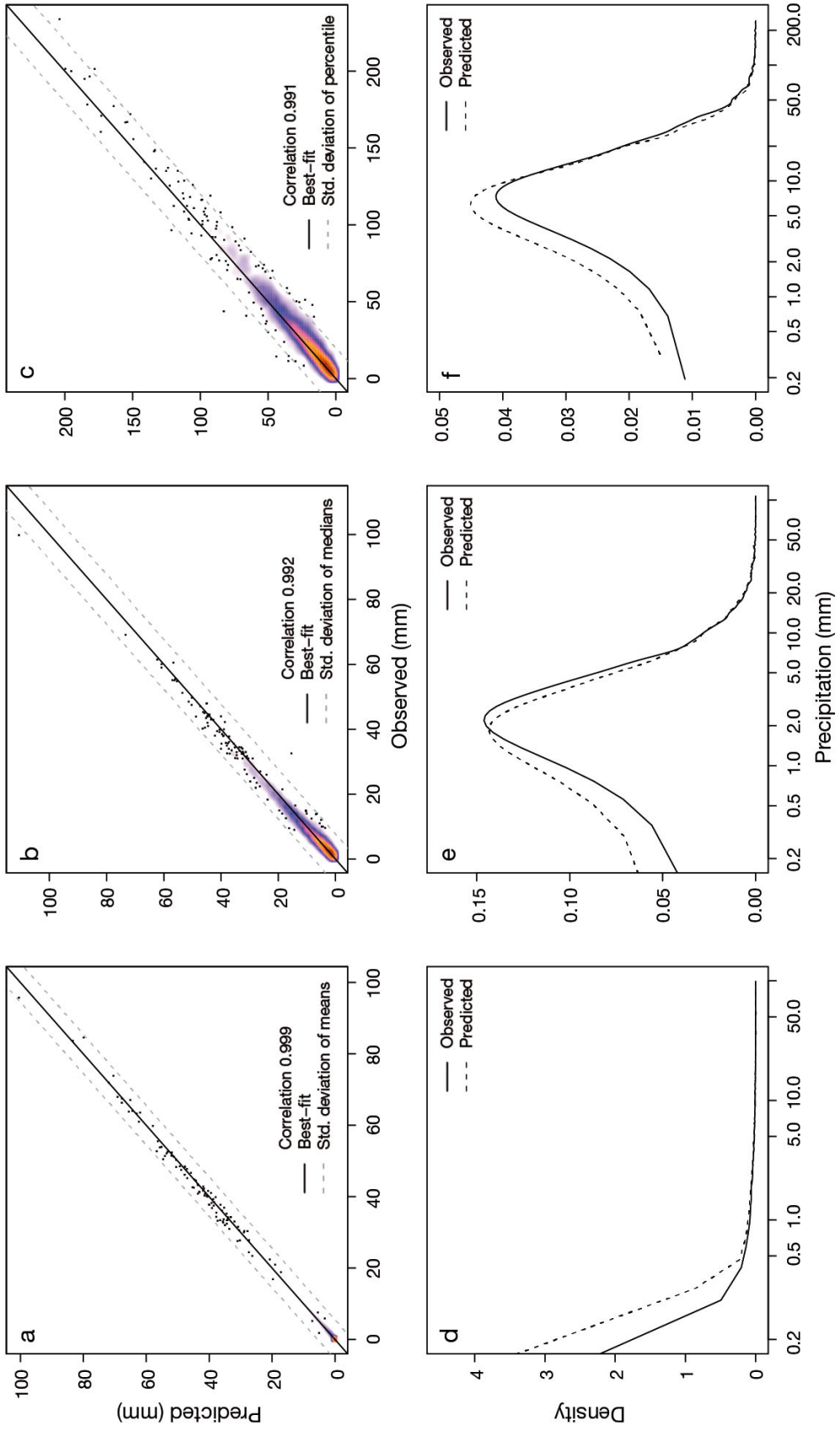

Fig. 7. Comparison of predicted reference values (RVs) and observed values, by days: (a) means of all available stations, considering all wet and dry days; (b) medians of all available stations, considering only wet days; (c) same as (b) but considering only days exceeding the 95th percentile of the wet days; (d–f) density curves corresponding to (a–c). Colours indicate the concentration of values from low (blue) to high (red)

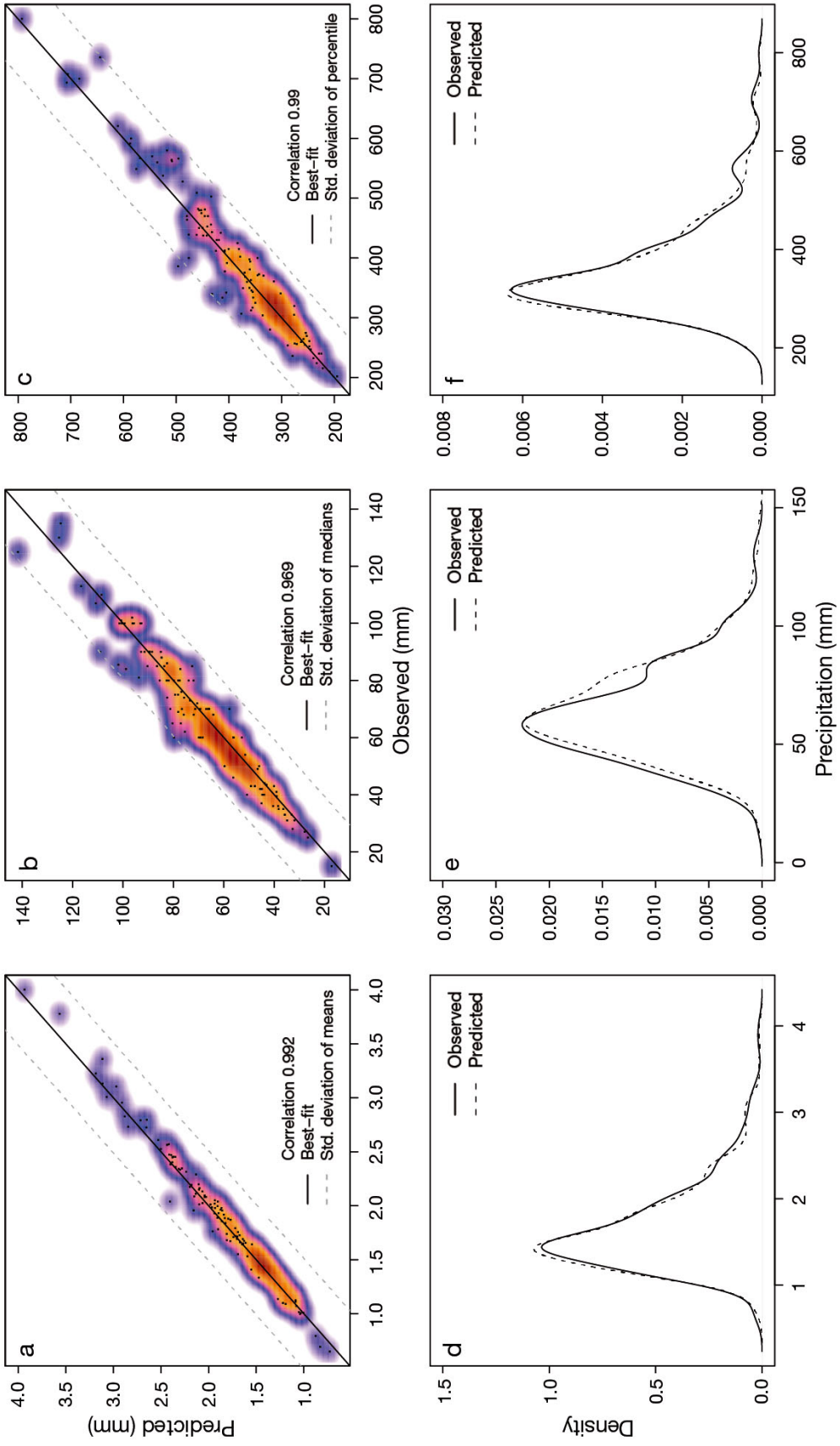

Fig. 8. Comparison of predicted reference values (RVs) and observed values, by stations: (a) means of all available days, considering all wet and dry days; (b) medians of all available days, considering only wet days; (c) same as (b), but considering only days exceeding the 95th percentile of the wet days; (d–f), density curves corresponding to (a–c)

Table 2. Statistics for each decile (1 to 10) and the range of values included in each one. %OBS, %PRED: percentage of total precipitation corresponding to each decile, in observed and predicted reference value (RV) data, respectively; MAE: mean absolute error; ME: mean error

Decile	Range (mm)	%OBS	%PRED	MAE (mm)	ME (mm)
1	>0–1.0	0.6	1.7	1.30	1.12
2	>1.0–2.0	1.6	2.6	1.65	1.08
3	>2.0–3.0	2.1	2.9	1.96	1.02
4	>3.0–4.4	3.2	4	2.28	0.91
5	>4.4–6.0	4.8	5.6	2.74	0.86
6	>6.0–8.4	6.5	7.1	3.23	0.72
7	>8.4–11.6	9	9.4	3.81	0.44
8	>11.6–16.5	12.6	12.6	4.69	0
9	>16.5–26.1	18.7	17.9	6.27	–0.89
10	>26.1	41	36.1	12.30	–5.45

error statistics of ME and MAE. The first groups (up to decile 7) represent less than 10% of the total precipitation in each class, and the values of MAE are higher than the range of their corresponding decile. MAE increased from low to high deciles with the inverse behaviour found in the ME statistics. In decile 8, the percentage of precipitation over the total is >10%, and the ME is 0. Decile 10 groups included values >26 mm, including 41% of the total precipitation in the observed values, and 36.1% in the predicted values. This decile has the highest MAE (12.30 mm) and the lowest ME (–5.45 mm).

The largest discrepancies between observed and estimated values occur in the lowest deciles (see Fig. S1 in the Supplement at www.int-res.com/articles/suppl/c073p167_supp.pdf), as shown in Table 2. The relative weight of the errors in precipitation totals in these ranges is low. These differences are due to the prediction of lower values of precipitation, also shown in daily means (Fig. 7d–f). Predicted values showed a smoother distribution than observed, which reveals stepped magnitudes (due to the observation ranges). The differences in the RM by stations did not show a defined spatial pattern over the study area (Fig. 9). Most of the stations were between 0.9 and 1.1. However, 19 of the 26 stations with overestimated means (RM > 1.10) were distributed along the northwest of the island, coinciding with elevated areas of the Tramuntana Range.

Monthly precipitation totals showed good agreement between observed and predicted values (Table 3). The best agreement corresponded with the summer months (June and July), with MAE values below 5 mm; while the highest MAE corresponded to autumn (October to December), coinciding with the highest mean rainfall amounts and the lowest ME.

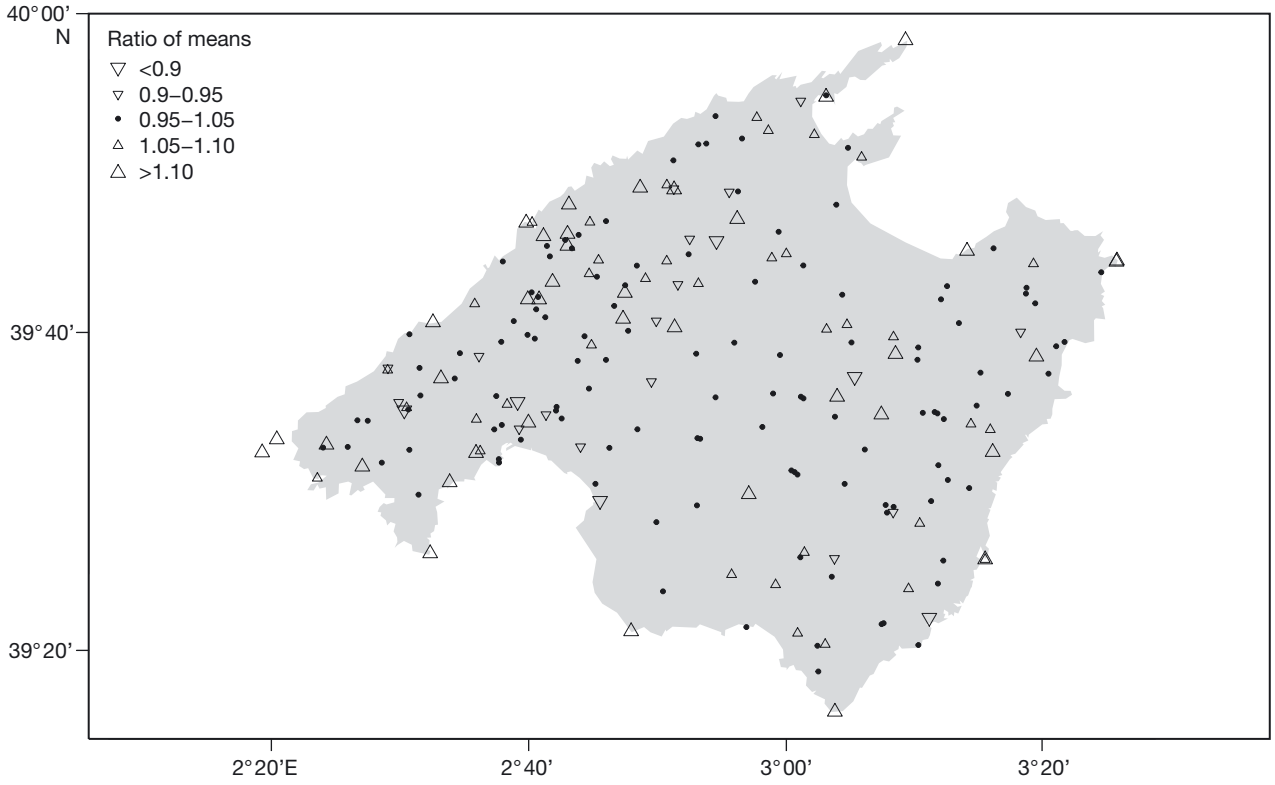

Fig. 9. Ratio of means (mean of estimations: mean of observations)

Table 3. Goodness-of-fit by month and the range of values included in each one. MAE: mean absolute error; ME: mean error; RM: ratio of means; RSD: ratio of standard deviations

	Range (mm)	MAE (mm)	ME (mm)	RM	RSD
Jan	0–407.2	8.17	0.65	1.01	1.01
Feb	0–428.0	7.10	0.27	1.01	1.02
Mar	0–408.1	6.99	0.42	1.01	1.00
Apr	0–429.0	7.93	0.45	1.01	1.01
May	0–365.5	7.26	0.26	1.01	1.01
Jun	0–172.0	4.16	0.09	1.01	1.01
Jul	0–213.0	2.75	0.03	1.00	1.01
Aug	0–244.0	6.38	0.08	1.00	1.02
Sep	0–430.0	12.45	0.39	1.01	1.00
Oct	0–478.0	13.29	1.08	1.01	1.01
Nov	0–687.5	14.21	–3.65	0.96	0.96
Dec	0–537.2	12.94	–3.49	0.95	0.96

Estimation of the mean and standard deviation of monthly totals showed no significant biases.

3.2.3. Gap filling

After the QC stage, the dataset contained 55.97% missing values over the 1971–2014 period. These missing values were imputed using the RVs, resulting in complete series after the reconstruction. An example of the gap filling process for one station (B_249) is given in Fig. 10. The time series show the original and reconstructed data at daily and monthly time scales. Correlation between observed and RVs (predictions on the same days and at the same locations as the observations) was very high in both cases (0.906 and 0.967 for daily and monthly values, respectively), and the density curves were also very similar (see Fig. S2 in the Supplement).

3.2.4. Inference

As an example of inference, a random pair of coordinates was selected (ETRS_89_UTM_30N X1016969, Y4410641, ALT 109m) corresponding to a location where no observations existed. Daily precipitation series and monthly and annual totals were estimated using data from nearby stations located at distances between 2 and 7 km (Fig. 11).

When applying the method for creating new data, as there are no observations with which to make direct comparisons, the standard error of the regression can be used as a measure of uncertainty. The shaded areas in Fig. 11 show the 95% prediction con-

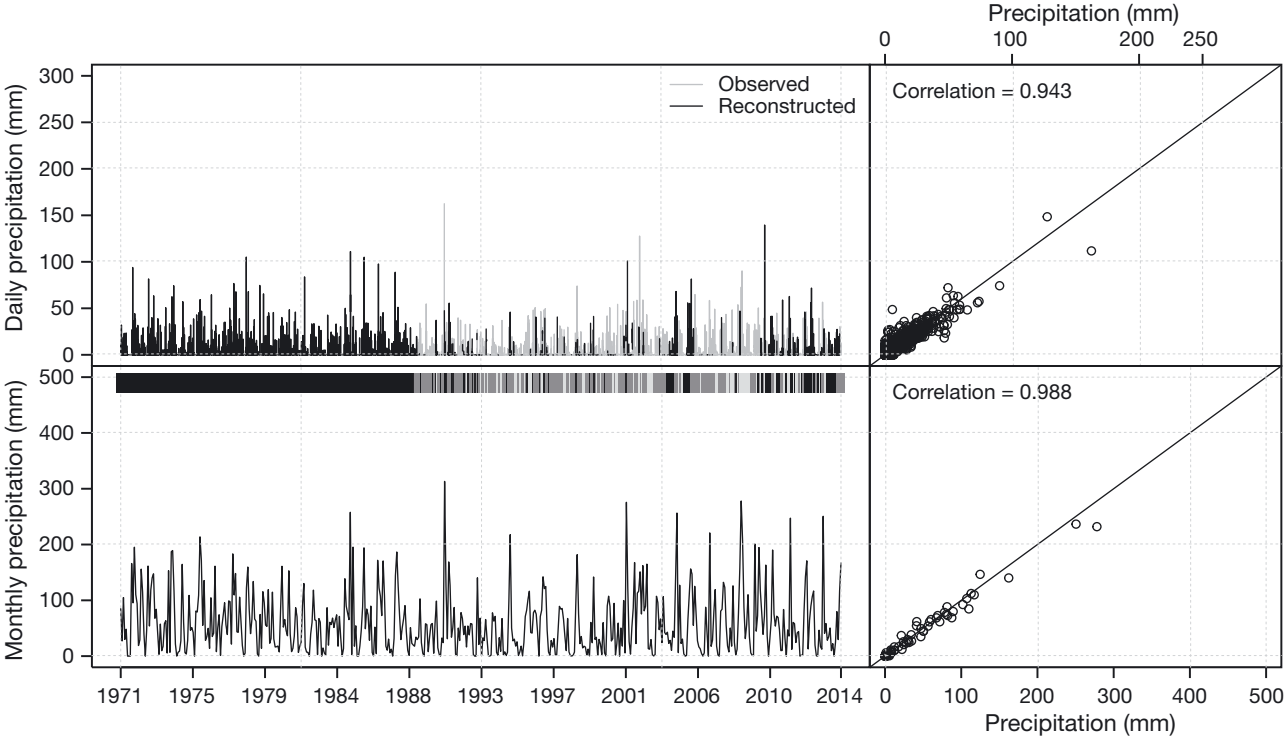

Fig. 10. Reconstruction of 'B249' observatory. Upper panel: time series of daily observed and reconstructed values and correlation between them; lower panel: time series of monthly observed and reconstructed totals (lines) with the information about the months when any missing value was filled (lines at top) and correlation between them

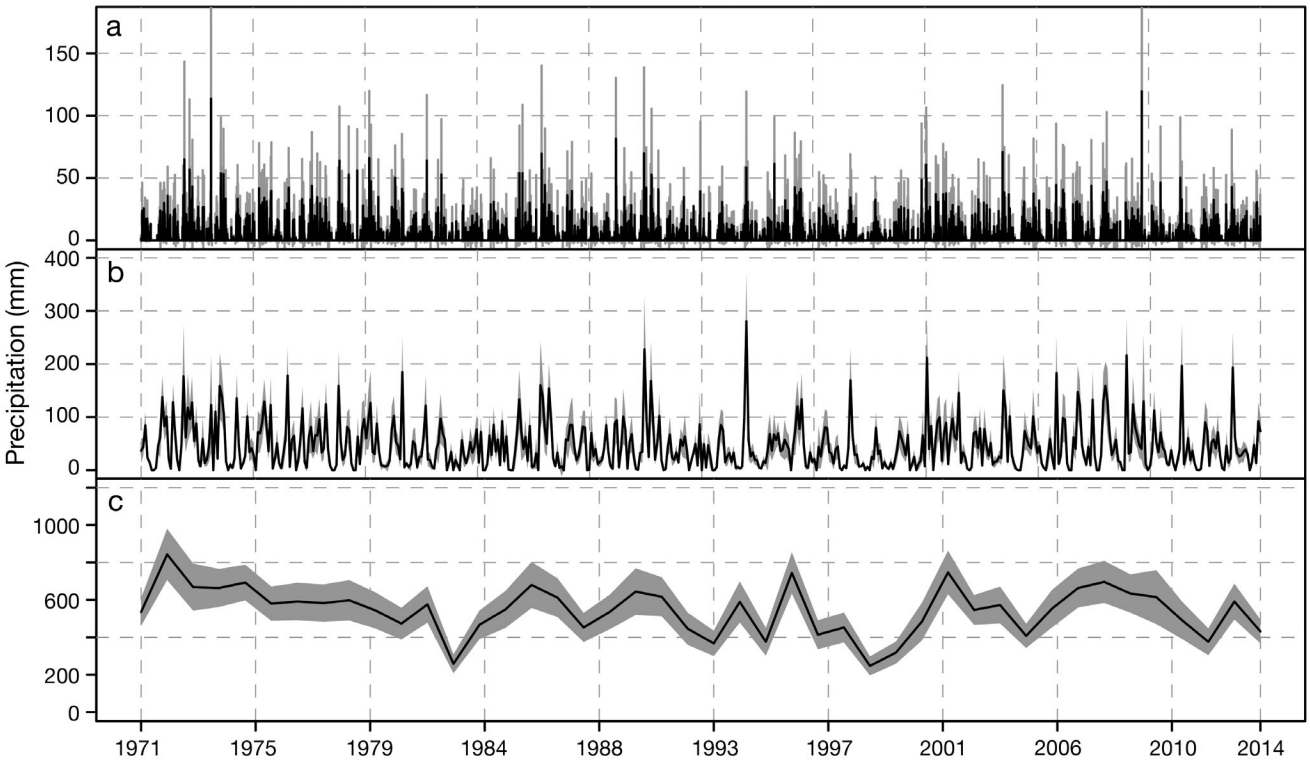

Fig. 11. Newly created series: (a) daily values; (b) monthly totals; (c) annual totals. Shaded areas: 95% confidence bands

fidence bands. As with the predicted magnitudes themselves, the prediction errors depend on the particular situation on each day, so 2 days with a similar predicted magnitude can have very different errors. Besides being informative, the uncertainty range can be used in further analyses or simulations to determine the uncertainty of computed variables by error propagation analysis.

Newly created data fit within the distribution function of their nearest stations at daily, monthly, and annual scales. Observed values showed similar variability between neighbouring stations, and predicted values faithfully reproduced precipitation behaviour at all temporal scales (see Fig. S3 in the Supplement).

The same procedure was applied to a set of regularly distributed points making up a grid covering Majorca with a spatial resolution of 1 km. Results are shown for annual precipitation and 5 extreme precipitation indices, showing a coherent spatial distribution of precipitation (Fig. 12). The final maps of climatic indices showed a high accuracy in spatial distribution of the variable. This is due to the use of all the available daily precipitation data and the independent estimation for each grid point and day, using the nearest observations to maintain the local variability of precipitation distribution.

The annual precipitation map (Fig. 12a) showed a clear south–north gradient from lower to higher values. The southern half of the island averaged lower values of annual accumulated precipitation, coinciding with the lower values of daily and extreme precipitation indices. Furthermore, the maximum length of dry spells (Fig. 12d) in this area exceeded 60 d, with the maximum length of wet events being <5 d. On the other hand, the north of the island, which corresponds to the most elevated zone, reached the highest values in annual totals, PMED, R20mm, RX1, and CWD (Fig. 12a,b,c,e,f, respectively).

4. DISCUSSION

Having a reliable and consistent daily precipitation dataset is key to any climatological study performing extreme events analysis, a study area characterisation, or to test relationships with other natural elements. For this reason, the method applied to obtain a quality-controlled and complete series should reflect the spatial and temporal variability of the variable of interest.

In the approach demonstrated here, the use of local models with 3 sources of variations (ALT, LAT, and

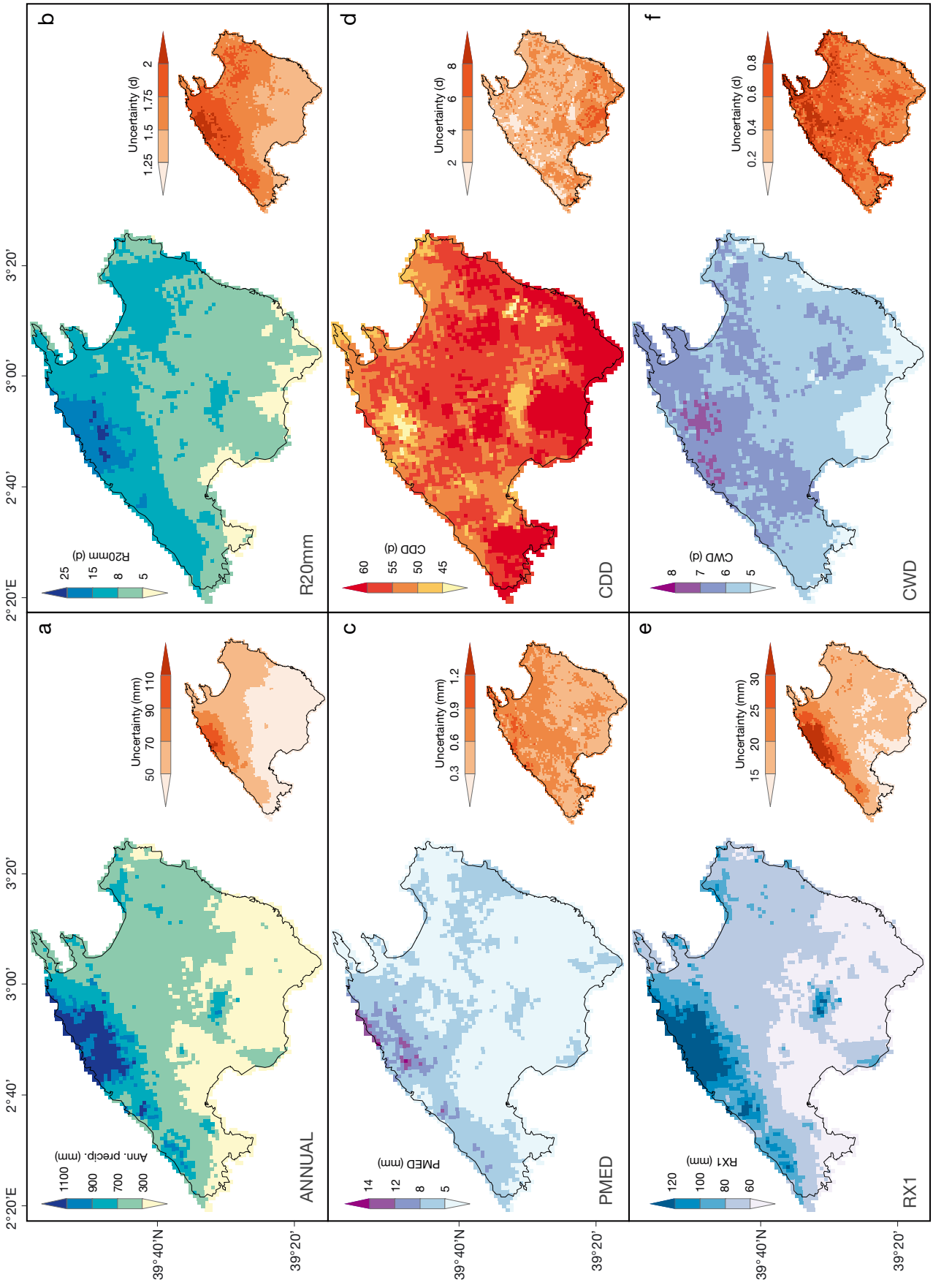

Fig. 12. Precipitation indices (left in each panel) and uncertainty of predictions (right in each panel) computed from the grid. (a) Annual precipitation, (b) number of days with precipitation over 20 mm (R20mm), (c) median of daily precipitation on wet days (PMED), (d) maximum consecutive dry days (CDD), (e) maximum precipitation in 1 d (RX1), and (f) maximum consecutive wet days (CWD)

LON) requires a minimum number of observations for each prediction. The use of fewer NNS could reduce the strength of the models and the predictions. Using only a few NNS makes contextualisation of the general precipitation situation difficult, and therefore the options for applying QC are reduced. On the other hand, the use of many more NNS will limit the desired local character of the predictions. For these reasons, 10 NNS were used, based on previous testing. This number allows for a contextualisation of the surrounding precipitation, and a model with 3 independent variables could in some cases represent real local conditions. However, this is not a magic number — it is a value that must be set according to the climatic characteristics of the study area and to the density of available observatories.

With respect to the set QC thresholds, isolated wet and dry days (QC.1 and QC.2) that could be real local elements were removed. Although these observations could be correct, they are related to less representative situations with respect to their environment, and in most cases, they corresponded to low precipitation values. On the other hand, the suspect dry and wet days (QC.4 and QC.5) could have also corresponded to real situations, but they did not fit the spatial distribution of local precipitation in their corresponding days. The same circumstance of unrepresentative observations was considered when removing outliers (QC.3). A ratio of 10 times over or under the predictions was used to eliminate the observed values, because most of these cases were related to problems of digitalisation or decimal errors. Any threshold used to remove observations is necessarily arbitrary. For this reason, the values used here are not necessarily adequate for all situations. These thresholds are user-defined and this method allows them to be flexibly defined.

4.1. RV versus RS

Most reconstruction methods rely on the statistical characteristics of the data over a long period of time, such as climatologies (long-term averages) or correlations between neighbouring stations. This imposes restrictions on data selection, since there is a minimum length required for any climatology or correlation to be reliable, and subsequently any data series shorter than this minimum length has to be discarded. Considering this restriction, an important proportion of the original data is not used in the final reconstruction, which represents a significant reduction in the information content of the process, and may even lead to spatial smoothing. A major advantage of the method described here is that all of the computations are done independently for each day and location, so there are no limitations on the use of all available observations, irrespective of their length. Daily and site-independent modelling also allows for a highly flexible reconstruction process, to adapt to the specific and changing characteristics of different days and sites.

GLMs were used for estimating the probability of wet day (i.e. BP) and the magnitude of precipitation (i.e. MP). These kinds of regressions have been used before for precipitation prediction (Hay et al. 2002, Helsel & Hirsch 2002, Syed et al. 2003, Hwang et al. 2012) using climatologies as independent variables. However, none of these studies used adaptive models for each location and time to represent the local precipitation variability as fully as possible.

Simolo et al. (2010) used a similar 2-step method using a Gamma-GLM and time-dependent regression coefficients for modelling the occurrence and magnitude of precipitation. Neykov et al. (2014) also separated the precipitation occurrence and intensity, but in their work, which is based on that of Furrer & Katz (2008), they fitted a hybrid Gamma-generalised Pareto (GP) and a hybrid Weibull-GP distribution to the whole data series to improve previous methods, which in most cases underestimated heavy precipitation values. Wong et al. (2014) used logistic models to predict wet/dry days and a mixture of probability distributions over the whole series for precipitation intensities, and Hwang et al. (2012) used a 2-step approach with a logistic regression to compute the spatial occurrence of precipitation, but using different interpolation methods to estimate precipitation amounts that also considered the monthly climatologies. Moncho et al. (2012) did not separate precipitation occurrence from intensity, and used a model with 4 parameters to predict the probability of precipitation with best results on wet days rather than dry days. Other works used a similar approach. This is, for instance, the case for Verdin et al. (2015), who used all the historical occurrence observations to fit a probit model to estimate the local coefficients, and then set the spatial structure through the empirical correlation of these probit models' errors. This required a minimum length of data series to apply the models, and, furthermore, they did not estimate precipitation amounts. These problems also affected Kleiber et al. (2012), who estimated the precipitation occurrence with a Gaussian process based on a spatiotemporal approach. Finally, Clark & Slater (2006) set the precipitation occurrence using the conditional

cumulative distribution function of each series and the precipitation intensity based on ensemble grids by using realisations from correlated random fields. Although they estimated the error term, it was incorporated into the final predictions, while in the method presented here it was provided separately as a measure of uncertainty.

However, despite the similarities, all these approaches were based on using the complete data series of the candidate and neighbouring stations, assuming that the relationship between them remains constant over time. Apart from this assumption, which may not hold for daily data, they require a minimum length of both data series and a minimum overlapping period between them in order for this relationship to be captured. In contrast, the method used in this study treats each daily record independently from the rest of the series. One direct advantage is that no overlapping or minimum data lengths are required and also, perhaps more importantly, it avoids assumptions of stationarity of the relationship between candidate and neighbouring series. At the daily scale this is important because the relationships between any 2 stations (e.g. one station registering higher precipitation than the other due to exposure to the dominant winds) may change dramatically from one day to the next due to changing meteorological conditions.

4.2. Estimation thresholds

The setting of a lower and an upper limit for each daily prediction by using an adaptive asymptote based on the data recorded at neighbouring stations prevented overshooting predictions, especially at high elevations where all observations occur at lower altitudes than that of the candidate location. This is a common problem in data prediction, as noted by Daly et al. (1994, 2008) when using standard linear regression. By using a quasi-binomial GLM and setting reasonable upper and lower limits to the predictions, overestimation was minimised while being able to estimate precipitation at altitudes (and latitudes and longitudes) outside the range of the observations. However, by changing the thresholds imposed to set the asymptotes, the predictions would change, especially in extreme situations where the candidate location is out of range of any of the covariates (latitude, longitude, or altitude) and extrapolation occurs. Thresholds were selected that kept estimated magnitudes within a range compatible with the observations. However, in datasets with larger differences between available stations these thresholds should probably be changed to increase the variability in estimations.

4.3. Quality control improvements and limitations

The process of identifying and removing suspect data was made only considering the observed precipitation and the influence of geographic variables, and was not based on the correlation structure of the stations in the long-term, nor on departures from computed climatologies. The 5 criteria used were adapted to the climatic behaviour of Mediterranean areas, but other settings could be used in other climates or geographical and data settings.

Among the studies reporting QC of daily precipitation data (Reek et al. 1992, Griffiths et al. 2003, Feng et al. 2004, Hubbard et al. 2005, Vicente-Serrano et al. 2010, Piccarreta et al. 2013), only a few gave final percentages of removed data even though the study area, the station density, and the number of observations were different from this research in each case. Using the present method, 1.59% of the original data were flagged by the 5 criteria and removed prior to further analysis. This value is similar to the 1.04% maximum proportion of data rejected in any one series registered by Vicente-Serrano et al. (2010) and to the 2% of data flagged as erroneous by Hubbard et al. (2005), but far more than the 0.04% suspect data of Reek et al. (1992). These authors dedicated the most criteria to temperature and only considered whether the daily precipitation values were inside predefined limits, and the relation with snowfall and snow depth data. Feng et al. (2004) found a very low figure of suspect data (0.02%), which may be at least partially attributed to their use of a highly-correlated series. Nonetheless, the percentage of flagged data will depend ultimately on how restrictive the thresholds used during the QC stage are. For instance, more permissive thresholds (lower required probability of precipitation occurrence or higher ratios to detect outliers) will result in a lower flagging of suspect data at the cost of increasing the probability of leaving problematic data un-flagged. It is important to set appropriate thresholds (using the proper criteria) adapted to the climate behaviour of the study area. The threshold values used here aimed not only to remove erroneous data but also anomalous observations that could have a negative effect (excess leverage) on the reconstruction of other series or on the construction of the grid. Observations that could be considered as outliers with respect to their neighbours will have a negative effect

on the attribution process, since they will have an excessive influence on the models, known as leverage. By removing these observations from further processing, it is possible to attain more robust estimations at the expense of smoothing the predicted spatial field. However, it is unlikely to remove original data corresponding to extreme events because the QC criteria are applied individually for each day, considering the nearest observations, with adaptive thresholds based on the input data. A compromise between detection of suspect data and maintaining the original variability of the data is therefore required. The values used in this work ensured that the vast majority of the local variability in precipitation was retained and that only very exceptional situations were removed.

4.4. Reconstruction and inference potential

The reconstruction of original data series and the creation of new ones make the method described here a useful tool to any user that needs to estimate precipitation data at a specific location. The creation of new series is a key factor in developing climatologies in new locations that could support other studies that do not depend on the availability of daily data for any location and period. In reference to gridded datasets, the method is able to estimate new data at any spatial resolution, always considering that the result is not a continuous surface of precipitation data over the territory but predictions at specific locations. Moreover, functions based on the latitude, longitude, and altitude of the 10 nearest observations are able to capture local variability, which may change from one day to the next. Ensor & Robeson (2008) found that while gridding increased the frequency of low-precipitation events, the frequency of heavy precipitation was greatly reduced. Beguería et al. (2015) highlighted that most gridding methods result in a reduction of the variance with respect to the observed data. This method, aimed at retaining local variability, may help in reducing this smoothing effect associated with other gridding methods. The examples of the applications in the present work show that, despite the daily precipitation estimations being computed independently for each grid point, the construction of different climatologies and extreme precipitation indices produced coherent spatial patterns and, as an improvement over other methods, the improvement in accuracy is noticeable. This would be impossible to detect without using all the available information and considering local variability of precipitation.

5. CONCLUSIONS

This study describes a spatially-based method for quality control, gap filling, and inference of daily precipitation data.

In the first phase, a prediction of the probability of precipitation occurrence (BP) was computed by binomial GLM against altitude, longitude, and latitude data using information from the 10 NNS. Then, the MP was calculated using quasi-binomial GLM, after rescaling the data of the NNS to a range between 0 and 1 to reduce the risk of over-shooting predictions in out-of-range situations. A combination of BP and MP resulted in the final RV for each location and day.

To flag suspect data, the RV values were compared with their corresponding observations, which were flagged according to 5 criteria aimed at detecting (1) isolated wet conditions, (2) isolated dry conditions, (3) suspect outliers, (4) suspect wet days, and (5) suspect dry days. In the final stage, RVs were computed again with the clean dataset after removing all suspect data to reconstruct a complete daily precipitation dataset that was used to calculate a 1 × 1 km spatial resolution grid over Majorca island.

Many examples of the application of this procedure to the reconstruction of a fragmentary station-based dataset are shown here, with satisfactory results in terms of goodness-of-fit and errors, bias, distribution density, monthly and annual totals, and daily and extreme precipitation indices. The potential for inference of daily precipitation at ungauged locations, and for grid construction, was also shown. In addition to the expected data, the method estimates the uncertainty of the predictions, which is also locally variable and may change from day to day.

Acknowledgements. This study was supported by research projects CGL2012-31668, CGL2015-69985-R, CGL2011-24185 and CGL2014-52135-C3-1-R, financed by the Spanish Ministerio de Economía y Competitividad (MINECO) and FEDER-ERDF funds. The researchers were supported by the Government of Aragón through the 'Programme of research groups' (groups H38, 'Clima, Cambio Global y Sistemas Naturales' and 'E68, Geomorfología y Cambio Global').

LITERATURE CITED

Alexander L, Zhang X, Peterson T, Caesar J and others (2006) Global observed changes in daily climate extremes of temperature and precipitation. J Geophys Res 111:D05109

Becker A, Finger P, Meyer-Christoffer A, Rudolf B, Schamm K, Schneider U, Ziese M (2013) A description of the global land-surface precipitation data products of the Global Precipitation Climatology Centre with sample

applications including centennial (trend) analysis from 1901–present. Earth Syst Sci Data 5:71–99
Beguería S, Angulo-Martínez M, López-Moreno JI, El-Kenawy AE, Vicente-Serrano S (2011) Assessing trends in extreme precipitation by non-stationary peaks-over-threshold analysis, NE Spain 1930–2006. Int J Climatol 31:2102–2114
Beguería S, Vicente-Serrano SM, Tomás-Burguera M, Maneta M (2015) Bias in the variance of gridded data sets leads to misleading conclusions about changes in climate variability. Int J Climatol 36:3413–3422
Caramelo L, Manso MD (2007) A study of precipitation variability in the Duero Basin (Iberian Peninsula). Int J Climatol 27:327–339
Castro L, Gironás J, Fernández B (2014) Spatial estimation of daily precipitation in regions with complex relief and scarce data using terrain orientation. J Hydrol (Amst) 517:481–492
Chaney NW, Sheffield J, Villarini G (2014) Development of a high-resolution gridded daily meteorological dataset over sub-Saharan Africa: spatial analysis of trends in climate extremes. J Clim 27:5815–5835
Clark MP, Slater AG (2006) Probabilistic quantitative precipitation estimation in complex terrain. J Hydrometeorol 7: 3–22
Daly C, Neilson RP, Phillips DL (1994) A statistical-topographic model for mapping climatological precipitation over mountainous terrain. J Appl Meteorol 33:140–158
Daly C, Gibson WP, Taylor GH, Johnson GL, Pasteris P (2002) A knowledge-based approach to the statistical mapping of climate. Clim Res 22:99–113
Daly C, Halbleib M, Smith J, Gibson W and others (2008) Physiographically sensitive mapping of climatological temperature and precipitation across the conterminous United States. Int J Climatol 28:2031–2064
Easterling DR, Meehl GA, Parmesan C, Changnon SA, Karl TR, Mearns LO (2000) Climate extremes: observations, modeling, and impacts. Science 289:2068–2074
Eischeid JK, Pasteris PA, Diaz HF, Plantico MS, Lott NJ (2000) Creating a serially complete, national daily time series of temperature and precipitation for the western United States. J Appl Meteorol 39:1580–1591
Ensor L, Robeson S (2008) Statistical characteristics of daily precipitation: comparisons of gridded and point datasets. J Appl Meteorol Climatol 47:2468–2476
Feng S, Hu Q, Qian W (2004) Quality control of daily meteorological data in China, 1951–2000: a new dataset. Int J Climatol 24:853–870
Frei C, Schär C (1998) A precipitation climatology for the Alps from high-resolution rain-gauge observations. Int J Climatol 18:873–900
Furrer E, Katz R (2008) Improving the simulation of extreme precipitation events by stochastic weather generators. Water Resour Res 44:W12439
González-Hidalgo JC, Brunetti M, de Luis M (2011) A new tool for monthly precipitation analysis in Spain: MOPREDAS database (monthly precipitation trends December 1945–November 2005). Int J Climatol 31: 715–731
Griffiths GM, Salinger MJ, Leleu I (2003) Trends in extreme daily rainfall across the South Pacific and relationship to the South Pacific converge zone. Int J Climatol 23: 847–869
Hay LE, Clarck MP, Wilby RL (2002) Use of regional climate model output for hydrologic simulations. J Hydrometeorol 3:571–590
Haylock M, Hofstra N, Tank A, Klok E, Jones P, New M (2008) A European daily high-resolution gridded data set of surface temperature and precipitation for 1950–2006. J Geophys Res 113:D20119
Helsel DR, Hirsch RM (2002) Statistical methods in water resources. Techniques of water-resources investigations, Book 4, Chapter A3. US Geological Survey, Washington, DC
Herrera S, Gutiérrez J, Ancell R, Pons M, Frías M, Fernández J (2012) Development and analysis of a 50-year high-resolution daily gridded precipitation dataset over Spain (Spain02). Int J Climatol 32:74–85
Hijmans RJ, Cameron SE, Parra JL, Jones PG, Jarvis A (2005) Very high resolution interpolated climate surfaces for global land areas. Int J Climatol 25:1965–1978
Hubbard KG, Goddard S, Sorensen WD, Wells N, Osugi TT (2005) Performance of quality assurance procedures for an applied climate information system. J Atmos Ocean Technol 22:105–112
Hwang Y, Clark M, Rajagopalan B, Leavesley G (2012) Spatial interpolation schemes of daily precipitation for hydrologic modeling. Stochastic Environ Res Risk Assess 26:295–320
Kleiber W, Katz RW, Rajagopalan B (2012) Daily spatiotemporal precipitation simulation using latent and transformed Gaussian processes. Water Resour Res 48:W01523
Klein-Tank AMG, Wijngaard JB, Können GP, Böhm R and others (2002) Daily dataset of 20th-century surface air temperature and precipitation series for the European Climate Assessment. Int J Climatol 22:1441–1453
Klok E, Klein-Tank A (2009) Updated and extended European dataset of daily climate observations. Int J Climatol 29:1182–1191
Lawrimore JH, Menne MJ, Gleason BE (2011) An overview of the Global Historical Climatology Network monthly mean temperature data set, version 3. J Geophys Res 116:D19121
Li Q, Zhang H, Liu X, Chen J, Li W (2009) A mainland China homogenized historical temperature dataset of 1951–2004. Bull Am Meteorol Soc 90:1062–1065
López-Moreno JI, Vicente-Serrano SM, Angulo-Martínez M, Beguería S, Kenawy A (2010) Trends in daily precipitation on the northeastern Iberian Peninsula, 1955–2006. Int J Climatol 30:1026–1041
Menne MJ, Durre I, Vose RS, Gleason BE, Houston TG (2012) An overview of the global historical climatology network-daily database. J Atmos Ocean Technol 29: 897–910
Min SK, Zhang K, Zwiers FW, Hegerl GC (2011) Human contribution to more-intense precipitation extremes. Nature 470:378–381
Mitchell TD, Jones PD (2005) An improved method of constructing a database of monthly climate observations and associated high-resolution grids. Int J Climatol 25: 693–712
Moncho R, Caselles V, Chust G (2012) Alternative model for precipitation probability distribution: application to Spain. Clim Res 51:23–33
New M, Hulme M, Jones PD (1999) Representing twentieth-century space-time climate variability. I. Development of a 1961–90 mean monthly terrestrial climatology. J Clim 12:829–856
New M, Hulme M, Jones PD (2000) Representing twentieth century space-time climate variability. II. Development

of 1901–1996 monthly grids of terrestrial surface climate. J Clim 13:2217–2238
New M, Lister D, Hulme M, Makin I (2002) A high-resolution data set of surface climate over global land areas. Clim Res 21:1–25
Neykov N, Neytchev P, Zucchini W (2014) Stochastic daily precipitation model with a heavy-tailed component. Nat Hazards Earth Syst Sci 14:2321–2335
Ninyerola M, Pons X, Roure JM (2007) Monthly precipitation mapping of the Iberian Peninsula using spatial interpolation tools implemented in a Geographic Information System. Theor Appl Climatol 89:195–209
Norrant C, Douguédroit A (2006) Monthly and daily precipitation trends in the Mediterranean (1950–2000). Theor Appl Climatol 83:89–106
Orlowsky B, Sereviratne SI (2012) Global changes in extreme events: regional and seasonal dimension. Clim Change 110:669–696
Perry M, Hollis D (2005) The generation of monthly gridded datasets for a range of climatic variables over the UK. Int J Climatol 25:1041–1054
Piccarreta M, Pasini A, Capolongo D, Lazzari M (2013) Changes in daily precipitation extremes in the Mediterranean from 1951 to 2010: the Basilicata region, southern Italy. Int J Climatol 33:3229–3248
R Core Team (2016) R: a language and environment for statistical computing. R Foundation for Statistical Computing, Vienna
Reek T, Doty SR, Owen TW (1992) A deterministic approach to the validation of historical daily temperature and precipitation data from the cooperative network. Bull Am Meteorol Soc 73:753–762
Río S, Herrero L, Fraile R, Penas A (2011) Spatial distribution of recent rainfall trends in Spain (1961–2006). Int J Climatol 31:656–667
Schneider U, Becker A, Finger P, Meyer-Christoffer A, Ziese M, Rudolf B (2014) GPCC's new land surface precipitation climatology based on quality-controlled in situ data and its role in quantifying the global water cycle. Theor Appl Climatol 115:15–40
Serrano-Notivoli R, de Luis M, Beguería S (2017) An R package for daily precipitation climate series reconstruction. Environ Model Softw 89:190–195
Simolo C, Brunetti M, Maugeri M, Nanni T (2010) Improving estimation of missing values in daily precipitation series by a probability density function-preserving approach. Int J Climatol 30:1564–1576
Su-Ping N, Yong L, Wei-Ping L, Tong-Wen W, Xue-Li S, Zai-Zhi W (2012) Quality control and analysis of global gauge-based daily precipitation dataset from 1980 to 2009. Adv Clim Chang Res 3:45–53
Sumner G, Ramis C, Guijarro JA (1995a) Daily rainfall domains in Mallorca. Theor Appl Climatol 51:199–221
Sumner G, Guijarro JA, Ramis C (1995b) The impact of surface circulation on significant daily rainfall patterns over Mallorca. Int J Climatol 15:673–696
Syed K, Goodrich D, Myers D, Sorooshian S (2003) Spatial characteristics of thunderstorm rainfall fields and their relation to runoff. J Hydrol (Amst) 271:1–21
Trenberth K (2011) Changes in precipitation with climate change. Clim Res 47:123–138
Trenberth K, Dai A, van der Schrier G, Jones PD, Barichivich J, Briffa KR, Sheffield J (2014) Global warming and changes in droughts. Nat Clim Chang 4:17–22
Verdin A, Rajagopalan B, Kleiber W, Katz RW (2015) Coupled stochastic weather generation using spatial and generalized linear models. Stochastic Environ Res Risk Assess 29:347–356
Vicente-Serrano S, Beguería S, López-Moreno J, García-Vera M, Stepanek P (2010) A complete daily precipitation database for northeast Spain: reconstruction, quality control, and homogeneity. Int J Climatol 30: 1146–1163
Wong G, Maraun D, Vrac M, Widmann M, Eden J, Kent T (2014) Stochastic model output statistics for bias correcting and downscaling precipitation including extremes. J Clim 27:6940–6959
Yatagai A, Kamiguchi K, Arakawa O, Hamada A, Yasutomi N, Kitoh A (2012) APHRODITE: constructing a long-term daily gridded precipitation dataset for Asia based on a dense network of rain gauges. Bull Am Meteorol Soc 93: 1401–1415
Zhang X, Alexander L, Hegerl G, Jones P and others (2011) Indices for monitoring changes in extremes based on daily temperature and precipitation data. WIREs Clim Chang 2:851–870
Zwiers FW, Alexander LV, Hegerl GC, Knutson TR and others (2013) Climate extremes: challenges in estimating and understanding recent changes in the frequency and intensity of extreme climate and weather events. In: Asrar GR, Hurrell JW (eds) Climate science for serving society. Springer, Dortrecht, p 339–389

Editorial responsibility: Balaji Rajagopalan, Boulder, Colorado, USA

Submitted: July 26, 2016; Accepted: May 25, 2017
Proofs received from author(s): July 27, 2017